THE JOURNAL OF BIOLOGICAL CHEMISTRY VOL. 284, NO. 13, pp. 8247–8255, March 27, 2009

AMP-activated Protein Kinase Phosphorylates R5/PTG, the Glycogen Targeting Subunit of the R5/PTG-Protein Phosphatase 1 Holoenzyme, and Accelerates Its Down-regulation by the Laforin-Malin Complex*[S]

Received for publication, November 7, 2008, and in revised form, January 21, 2009 Published, JBC Papers in Press, January 26, 2009, DOI 10.1074/jbc.M808492200

Santiago Vernia[‡], M. Carmen Solaz-Fuster[‡], José Vicente Gimeno-Alcañiz[‡], Teresa Rubio[‡], Luisa García-Haro[‡], Marc Foretz[§], Santiago Rodríguez de Córdoba[¶], and Pascual Sanz[‡1]

From the [‡]Instituto de Biomedicina de Valencia, Consejo Superior de Investigaciones Científicas (CSIC) and CIBER de Enfermedades Raras (CIBERER), Jaime Roig 11, Valencia 46010, Spain, the [§]Institut Cochin, Université Paris Descartes, CNRS (UMR 8104) and INSERM U567, Paris 75014, France, and the [¶]Centro de Investigaciones Biológicas, CIBERER, Ramiro de Maeztu 9, Madrid 28040, Spain

R5/PTG is one of the glycogen targeting subunits of type 1 protein phosphatase, a master regulator of glycogen synthesis. R5/PTG recruits the phosphatase to the places where glycogen synthesis occurs, allowing the activation of glycogen synthase and the inactivation of glycogen phosphorylase, thus increasing glycogen synthesis and decreasing its degradation. In this report, we show that the activity of R5/PTG is regulated by AMP-activated protein kinase (AMPK). We demonstrate that AMPK interacts physically with R5/PTG and modifies its basal phosphorylation status. We have also mapped the major phosphorylation sites of R5/PTG by mass spectrometry analysis, observing that phosphorylation of Ser-8 and Ser-268 increased upon activation of AMPK. We have recently described that the activity of R5/PTG is down-regulated by the laforin-malin complex, composed of a dual specificity phosphatase (laforin) and an E3-ubiquitin ligase (malin). We now demonstrate that phosphorylation of R5/PTG at Ser-8 by AMPK accelerates its laforin/malin-dependent ubiquitination and subsequent proteasomal degradation, which results in a decrease of its glycogenic activity. Thus, our results define a novel role of AMPK in glycogen homeostasis.

Glycogen homeostasis depends mainly on the activity of the enzymes involved in its synthesis (glycogen synthase (GS)[2]) and its degradation (glycogen phosphorylase). These activities are regulated by a complex mechanism involving both allosteric regulation and phosphorylation (1, 2). Interestingly, although there are several kinases (AMPK, PKA, CKI, and glycogen synthase kinase 3) that inhibit glycogen synthesis through the phosphorylation of GS, there is only one known phosphatase (type 1 protein phosphatase (PP1)) that dephosphorylates both GS (leading to its activation) and glycogen phosphorylase (leading to its inactivation), which results in glycogen accumulation (1, 2). PP1 is recruited to glycogen by a family of glycogen targeting proteins, including: G_M, G_L, R5/PTG, R6, and R3E (3–7). The regulation of the activity of the holoenzyme formed by the PP1 catalytic subunit and one of these glycogen targeting subunits is different in each case. The glycogenic activity of G_M is down-regulated by its PKA-dependent phosphorylation; PKA phosphorylates G_M at a site in its PP1 binding motif, which leads to its dissociation from PP1. The glycogenic activity of the G_L-PP1c holoenzyme is down-regulated by an allosteric mechanism involving phosphorylase-a (8–10). Little is known about the regulation of the holoenzymes involving R6 or R3E, but in the case of R5/PTG, we and others have recently described that its glycogenic activity is down-regulated by the laforin-malin complex, composed of a dual specificity phosphatase (laforin) and an E3-ubiquitin ligase (malin), which recognizes and ubiquitinates R5/PTG and targets it for proteasomal-dependent degradation (11–13).

Laforin and malin are two key proteins related to Lafora disease (LD, OMIM 254780), an autosomal recessive neurodegenerative disorder characterized by the presence of glycogen-like intracellular inclusions named Lafora bodies. Although the role of these two proteins in cellular physiology is still poorly understood, several reports indicate that both the enzymatic activity of each protein and the physical interaction between them are critical parameters for the pathogenesis of LD. The fact that one of the histological determinants that characterize LD is the accumulation of glycogen-like intracellular inclusions suggests a direct involvement of the laforin-malin complex in the regulation of glycogen biosynthesis (14).

* This work was supported by the Fundación Marato TV3, the Spanish Ministry of Education and Science (Grant SAF2005-00852), and the European Commission (Grant LSHM-CT-2004-005272). The costs of publication of this article were defrayed in part by the payment of page charges. This article must therefore be hereby marked "*advertisement*" in accordance with 18 U.S.C. Section 1734 solely to indicate this fact.

[S] The on-line version of this article (available at http://www.jbc.org) contains supplemental Fig. S1.

[1] To whom correspondence should be addressed. Tel.: 34-96-339-1779; Fax: 34-96-369-0800; E-mail: sanz@ibv.csic.es.

[2] The abbreviations used are: GS, glycogen synthase; AICAR, 5-aminoimidazole-4-carboxamide-1β-D-ribofuranoside; AMPK, AMP-activated protein kinase; CHX, cycloheximide; LD, Lafora disease; PKA, protein kinase A; PP1, type 1 protein phosphatase; PP1c, catalytic subunit of PP1; R5/PTG, protein targeting to glycogen R5; E3, ubiquitin-protein isopeptide ligase; CHO, Chinese hamster ovary; CMV, cytomegalovirus; HA, hemagglutinin; CHAPS, 3-[(3-cholamidopropyl)dimethylammonio]-1-propanesulfonic acid; MBP, maltose-binding protein; MS, mass spectrometry; MS/MS, tandem MS; MALDI-TOF, matrix-assisted laser desorption ionization time-of-flight; HPLC, high-performance liquid chromatography.

Contrary to mammalian cells, yeast glycogen synthesis is stimulated by nutrient limitation. However, the activity of yeast glycogen synthase (Gsy2) is similarly regulated by phosphorylation. The dephosphorylation and activation of Gsy2 is carried out mainly by the PP1 holoenzyme composed by Gac1 (glycogen-targeting subunit) and the phosphatase catalytic subunit Glc7 (15). It has been described that the Snf1 kinase (yeast orthologue of mammalian AMP-activated protein kinase (AMPK), see below) activates the Gac1/Glc7 protein phosphatase complex, thus facilitating the activation of Gsy2 under conditions of Snf1 activation (15, 16).

AMPK is a serine/threonine protein kinase that acts as a sensor of cellular energy status. Once activated, it switches on catabolic pathways and switches off many ATP-consuming processes (anabolic pathways) (see Refs. 17 and 18 for reviews). AMPK is a heterotrimer of three different subunits, α, β, and γ, each of which has different isoforms (α1, α2, β1, β2, γ1, γ2, and γ3). AMPKα is the catalytic subunit of the AMPK complex, AMPKγ is involved in AMP binding, and AMPKβ functions as a scaffold to assemble α and γ subunits and also determines the subcellular localization and substrate specificity of the complex (17, 18).

Because the yeast Snf1 orthologue of AMPK is involved in the regulation of the yeast PP1 holoenzyme involved in glycogen synthesis (Gac1/Glc7; see above), in this work we studied whether AMPK could regulate similar PP1 holoenzymes in mammalian cells. We found that AMPK interacted physically with the R5/PTG glycogen-targeting subunit and made it a better substrate for its laforin/malin-dependent degradation, resulting in a decrease of its glycogenic activity.

EXPERIMENTAL PROCEDURES

Cell Culture and Treatments—Chinese hamster ovary (CHO) and human embryonic kidney (Hek293) cells were grown in Ham's F-12 medium (Invitrogen) or Dulbecco's modified Eagle's medium (Lonza), respectively, supplemented with 100 units/ml penicillin, 100 μg/ml streptomycin, 2 mM glutamine, 10% inactivated fetal bovine serum (Invitrogen). 1.5×10^6 cells were plated onto 60-mm-diameter culture dishes the day before transfection. Cells were transfected with 1 μg of each plasmid using Lipofectamine 2000 (Invitrogen). When indicated, cycloheximide (100 μM) was added for different periods of time. Twenty-four hours after transfection, cells were scraped on ice in lysis buffer (10 mM Tris-HCl, pH 8, 150 mM NaCl, 15 mM EDTA, 0.6 M sucrose, 0.5% Nonidet P-40, Complete protease inhibitor mixture (Roche Applied Science), 1 mM phenylmethylsulfonyl fluoride, 50 mM NaF and 5 mM $Na_2P_2O_7$). Cells were lysed by repeated passage through a 25-gauge needle. Twenty-five micrograms of total protein from the soluble fraction of cell lysates was analyzed by SDS-PAGE and Western blotting using appropriate antibodies: mouse monoclonal anti-laforin (12), rabbit polyclonal anti-R5/PTG (raised against the synthetic peptide (GPYDEFQRRHFVNK) corresponding to amino acids 16–29 of the human R5/PTG), mouse monoclonal anti-HA (Sigma), mouse monoclonal anti-tubulin (Santa Cruz Biotechnology), or rabbit polyclonal anti-actin (Sigma) as in Ref. 12. Human primary skin fibroblasts, either from LD patients or healthy subjects (12), were cultured in Dulbecco's modified Eagle's medium-15% fetal bovine serum with the antibiotics and glutamine described above.

Plasmids—To construct plasmid pACT2-GM, a BglII fragment containing the rabbit G_M open reading frame from pcDNA3-FLAG-rabGM (19), a gift from Dr. D. L. Brautigan (Center for Cell Signaling, University of Virginia), was subcloned into pUC18; then, a BamHI/SalI fragment was subcloned into pACT2 (20). Plasmid pACT2-GL was obtained by subcloning into pACT2 a BamHI/SalI fragment of a PCR-amplified human G_L open reading frame using the Image Consortium clone 13484-G21 as a template. Plasmid pACT2-R5/PTG contained the human full-length R5/PTG open reading frame (21). Plasmids pACT2-R5/PTG (Ser-8 → Ala, Ser-8 → Asp, Ser-268 → Ala, and Ser-268 → Asp) were generated by subcloning the mutated R5/PTG fragments (described below), into pACT2 vector. A SfiI/BglII fragment from pACT2-R5/PTG wild type was subcloned into vector pCMV-HA (Clontech) to obtain plasmid pCMV-HA-R5/PTG. An 8×His tag was inserted into pCMV-HA-R5 by digestion with SfiI/SmaI and re-ligation with hybridized primers 5′-CACATCATCATCATCATCATCATGC-3′ and 5′-GCATGATGATGATGATGATGATGTGCCA-3′, yielding plasmid pCMV-HA-8×His-R5/PTG. To express R5/PTG in bacteria, we subcloned an EcoRI/SalI fragment containing the R5/PTG open reading frame into plasmid pMALC2 (New England Biolabs), which produces an N-terminal fusion of R5/PTG with the maltose-binding protein. Human PP1α was amplified by PCR from a human fetal liver cDNA library and cloned into BamHI/SalI sites of pBTM116, resulting in plasmid pBTM-PP1α.

Plasmids pcDNA3-AMPKα2 T172D (expressing a constitutively active form of AMPKα2), pcDNA3-AMPKβ2, and pcDNA3-AMPK γ1 were kindly provided by Dr. D. Carling (Cellular Stress Group, MRC Clinical Sciences Centre, Imperial College School of Medicine, Hammersmith Hospital, London). Other plasmids used in this study were pBTM-AMPKα2, pBTM-AMPKβ2, pBTM-AMPKγ1, and pCMV-Myc-AMPKα2 (22) and pEG202-laforin, pCMV-Myc-Laforin, and pcDNA-HA-Malin (12).

Site-directed Mutagenesis—Site-directed mutagenesis of R5/PTG constructs was performed using the QuikChange kit (Stratagene) and the following primers: (*a*) Ser-8 → Ala: forward, 5′-ATGAGGCTTTGCTTGGCACATGCACCACCTGTGAAGAGTTTCCTG-3′; reverse, 5′-CAGGAAACTCTTCACAGGTGGTGCATGTGCCAAGCAAAGCCTCAT-3′; (*b*) Ser-268 → Ala: forward, 5′-GTTAGAGTCAACAATCTTTGGCGCTCCGAGGCTGGCTAGTGGGCTCTTC-3′; reverse, 5′-GAAGAGCCCACTAGCCAGCCTCGGAGCGCCAAAGATTGTTGACTCTAAC-3′; (*c*) Ser-8 → Asp: forward, 5′-ATGAGGCTTTGCTTGGCACATGATCCACCTGTGAAGAGTTTCCTG-3′; reverse, 5′-CAGGAAACTCTTCACAGGTGGATCATGTGCCAAGCAAAGCCTCAT-3′; and (*d*) Ser-268 → Asp: forward, 5′-GTTAGAGTCAACAATCTTTGGCGATCCGAGGCTGGCTAGTGGGCTCTTC-3′; reverse, 5′-GAAGAGCCCACTAGCCAGCCTCGGATCGCCAAAGATTGTTGACTCTAAC-3′. Mutations and construct fidelity were confirmed by DNA sequencing.

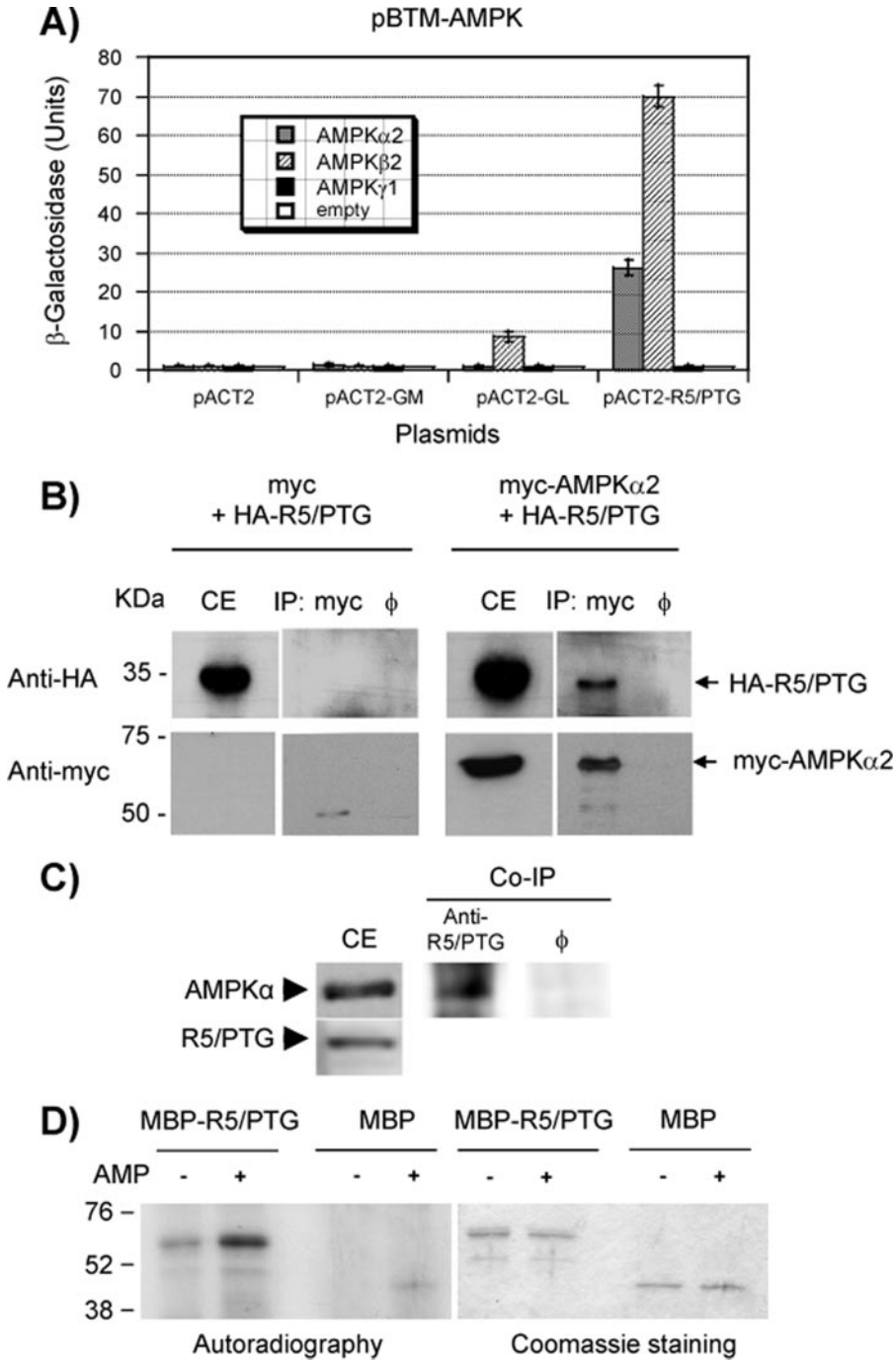

FIGURE 1. **AMPK interacts physically with R5/PTG.** *A*, yeast CTY10.5d cells transformed with plasmids pBTM116 (empty), pBTM-AMPKα2, pBTM-AMPKβ2, and pBTM-AMPKγ1 were co-transformed with plasmids pACT2 (empty), pACT2-GM, pACT2-GL, and pACT2-R5/PTG. Protein interaction was estimated using the yeast two-hybrid system, by measuring the β-galactosidase activity. Values correspond to means from four to six different transformants (*bars* indicate $\pm$ S.D.). *B*, AMPKα2 co-immunoprecipitates with R5/PTG. Protein extracts (300 μg) were prepared from Hek293 cells transfected with plasmids pCMV-Myc-AMPKα2 and pCMV-HA-R5/PTG. 1 μl of anti-Myc or pre-immune serum (ϕ) were used to immunoprecipitate the extracts (*IP*). Pelleted proteins were analyzed by SDS-PAGE and immunodetected with anti-HA (*upper panel*) and anti-Myc (*lower panel*) monoclonal antibodies. Proteins in the input crude extracts (*CE*, 30 μg) were also immunodetected with anti-HA and anti-Myc antibodies. *C*, interaction of endogenous R5/PTG and AMPKα. Crude extracts (1.5 mg) from mice skeletal muscle (see "Experimental Procedures") were immunoprecipitated with 1 μl of anti-R5/PTG antibodies or pre-immune serum (ϕ). Immunoprecipitates were analyzed by SDS-PAGE and Western blotting using anti-AMPKα antibodies. Proteins in the input crude extracts (*CE*, 50 μg) were also immunodetected with anti-AMPKα and anti-R5/PTG antibodies. *D*, AMPK phosphorylates a MBP-R5/PTG fusion protein *in vitro*. MBP-R5/PTG (50 ng) and MBP (100 ng), produced in bacteria were phosphorylated *in vitro* using 50 milliunits of AMPK (Upstate) and [γ-^{32}P]ATP, in the presence or absence of 300 μM AMP. Samples were analyzed by SDS-PAGE and autoradiography. Size standards are indicated in kilodaltons.

Laforin Small Interference RNA Silencing—The mammalian expression vector, pSUPER.neo.GFP (Oligoengine) was used for expression of laforin-specific small interference RNA in human Hek293 cells. Sense and antisense oligonucleotides corresponding to nucleotides 872–891 of human EPM2A cDNA (GenBank^{TM} accession number NM_005670) were annealed and subcloned into pSUPER.neo.GFP vector, resulting in plasmid pSUPER-laf.

Yeast Two-hybrid Analyses—The yeast CTY10.5d strain was co-transformed with combinations of pACT2-GM, pACT2-GL, and pACT2-R5/PTG and different pBTM-AMPKα2, pBTM-AMPKβ2, and pBTM-AMPKγ1 plasmids. To analyze the effect of phosphorylation of R5/PTG on its protein-protein interactions, plasmid pACT2-R5/PTG (wild type or S8A and S268A mutants) were co-transformed with pBTM-PP1α, pBTM-AMPKα2, pBTM-AMPKβ2, or pEG202-Laforin. Transformants were grown in selective SC medium, and β-galactosidase activity was assayed in permeabilized cells and expressed in Miller Units as in a previous study (23).

Co-immunoprecipitation Analysis—Human embryonic kidney cells (Hek293) transfected with plasmids pCMV-HA-R5/PTG and pCMV-Myc-AMPKα2 or with the corresponding empty plasmids were used for co-immunoprecipitation studies carried out as in a previous study (22). In the case of co-immunoprecipitation of endogenous proteins, crude extracts from mouse skeletal muscle (C57B6 mice) were prepared by homogenizing the samples with a tissue homogenizer in ice-cold lysis buffer containing 100 mM KCl, 25 mM Tris-HCl, pH 8, 10% glycerol, 0.5% Triton X-100, 5 mM NaF, 5 mM $Na_2P_2O_7$, 1 mM phenylmethylsulfonyl fluoride, 2 mM $NaVO_4$, and protease inhibitor mixture (Roche Applied Science) and then clarified by centrifugation at 5000 rpm, 5 min, at 4 °C. 1.5 mg of total protein from the soluble fraction was used

for immunoprecipitation using specific anti-R5/PTG antibody or pre-immune serum and protein A/G-plus agarose (Santa Cruz Biotechnology). Immunoprecipitates were analyzed by Western blotting using polyclonal anti-AMPKα antibody (Cell Signaling Technology).

Two-dimensional Electrophoresis—CHO cells were transfected with the corresponding plasmids and 24 h after transfection, extracts were made in urea lysis buffer (9.7 M urea, 4% CHAPS, 20 mM dithiothreitol). HA-R5/PTG was analyzed by two-dimensional electrophoresis using an IPGphor (Amersham Biosciences Bioscience, Uppsala, Sweden) instrument. For the first dimension (IEF), 50 μg of total protein (in 100 μl of 9.7 M urea, 4% CHAPS, 20 mM dithiothreitol and 0.5% IPG buffer) were loaded on a 7 cm IPG strip (pH range 6–11) using the following focusing conditions: 500 V for 30 min, 1000 V for 30 min and 5000 V for 80 min. Electrophoretic separation (second dimension) was performed in a SDS-PAGE.

λ-Phosphatase Treatment—CHO cell crude extracts (50 μg) in λ-phosphatase buffer containing 2 mM $MnCl_2$ were treated at 30 °C for 30 min with 50 units of λ-phosphatase (New England Biolabs). The reactions were stopped by adding two volumes of urea lysis buffer.

Expression of Recombinant MBP-R5/PTG in E. coli—*Escherichia coli* transformants harboring MBP-R5/PTG fusion were grown in 500 ml of LB/ampicillin. Transformants were grown at 37 °C until the absorbance at 600 nm reached a value of ~0.3. Isopropyl-β-D-thiogalactoside was then added to a concentration of 0.1 mM, and cultures were maintained overnight at 25 °C. Cells were harvested and resuspended in 20 ml of sonication buffer (50 mM Tris-HCl, pH 7.5, 150 mM NaCl, 0.2 mM EDTA, 10% glycerol, 0.1% Triton X-100, 2 mM dithiothreitol, 2 mM phenylmethylsulfonyl fluoride, and Complete protease inhibitor mixture (Roche Applied Science)). Cells were disrupted by sonication, and the fusion protein was purified by passing the extracts through a 1-ml bed volume of amylose-Sepharose columns (Sigma). MBP fusion proteins were eluted from the column with 50 mM maltose in a buffer containing 50 mM Tris-HCl, pH 7.5, 150 mM NaCl, and 15% glycerol. Samples were stored at −80 °C.

AMPK in Vitro Phosphorylation Assay—50 ng of purified MBP-R5/PTG fusion protein were phosphorylated with 50 milliunits AMPK (Upstate), in a final volume of 20 μl of a buffer containing 20 mM HEPES-NaOH, pH 7.0, 1 mM dithiothreitol, 10 mM $MgCl_2$, 300 μM AMP, and 100 μM of a mixture of [γ-^{32}P]ATP (3000 Ci/mmol) and cold ATP, following the manufacturer's instructions (Upstate). The reaction was incubated at 30 °C for 1 h and stopped by boiling the mixtures in sample buffer. Samples were analyzed by SDS-PAGE and autoradiography. 250 ng of MBP fusion proteins were analyzed by SDS-PAGE and stained with Coomassie Blue.

R5/PTG Purification and Mass Spectrometry—CHO cells were transfected with plasmid pCMV-HA-8×His-R5/PTG using Lipofectamine 2000. Cell lysates from 20 plates (100-mm-diameter plates) were used for purification of poly-His-tagged R5/PTG. Twenty-four hours after transfection, cells were harvested in lysis buffer (0.15 M NaCl, 10 mM Tris-HCl, pH 7.5, 15 mM EDTA, pH 8.0, 0.6 M sucrose, 50 mM NaF, 5 mM $Na_2P_2O_7$, 1 mM phenylmethylsulfonyl fluoride, and protease inhibitor mixture). Cell extracts were centrifuged at 8000 rpm for 20 min at 4 °C. The resulting pellet was resuspended in Buffer A (8 M urea, 250 mM NaCl, 100 mM Tris-HCl, pH 7.5, 0.1% Nonidet P-40) and then used for purification using a fast protein liquid chromatography AKTA system and a His-Trap column (Amersham Biosciences). Additionally, poly-His-tagged R5/PTG was purified from CHO cells infected with an adenovirus expressing a mutated form of AMPKγ1 subunit (R70Q) that renders a constitutively active AMPK complex. Purified samples were analyzed by SDS-PAGE electrophoresis and Coomassie staining. The band corresponding to HA-8×His-R5/PTG was excised and digested *in situ* with trypsin, and the resulting peptides were analyzed by MALDI-TOF/MS and HPLC-MS/MS. Proteomic analysis was performed at the Prince Felipe Research Centre (CIPF-Valencia, a node of the Spanish ProteoRed network). MALDI-TOF/MS and HPLC-MS/MS data were analyzed with the bioinformatics database system Mascot (Matrix Sciences, London), and Paragon (ProteinPilot^{TM}). These data confirmed the identity of the purified protein. Ion fragmentation analysis assigned Ser-8 and Ser-268 as the phosphorylated residues within the R5/PTG sequence. Comparative analysis of HPLC-MS/MS data using Decyder MS software showed that Ser-8 and Ser-268 were quantitatively more phosphorylated when purified in the presence of a constitutively active AMPK.

Glycogen Determination—Glycogen determination in transfected Hek293 cells was carried out as in a previous study (24).

Statistical Data Analysis—Data are expressed as means ± S.D. Statistical significance of differences between the groups was evaluated by a paired Student's *t* test with two-tailed distribution. The significance has been considered at $p < 0.05$ (*), $p < 0.01$ (**), and $p < 0.001$ (***), as indicated in each case.

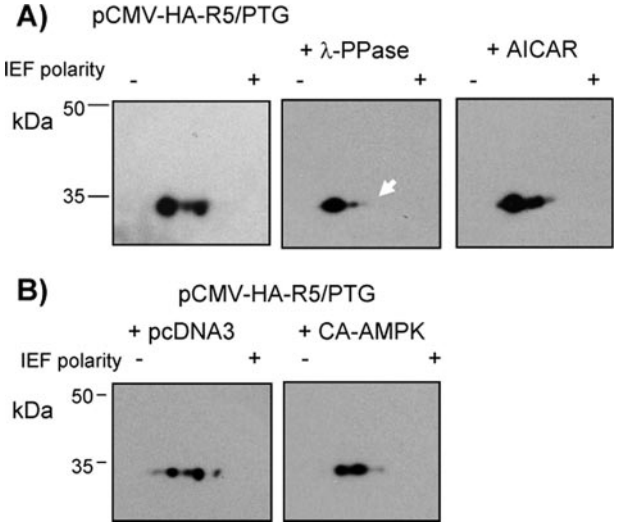

FIGURE 2. **AMPK phosphorylates R5/PTG *in vivo*.** *A*, cell extracts from CHO cells transfected with plasmid pCMV-HA-R5/PTG were analyzed by two-dimensional electrophoresis and Western blotting using anti-HA monoclonal antibodies (*left panel*). An aliquot of these extracts was previously treated with λ-phosphatase (*middle panel*). Cell extracts from CHO cells treated with AICAR (0.5 mM, 6 h) were analyzed similarly (*right panel*). *B*, CHO cells were co-transfected with plasmid pCMV-HA-R5/PTG and either a combination of plasmids that reconstituted a constitutively active form of the AMPK complex (pcDNA3-AMPKα2 T172D, pcDNA3-AMPKβ2, and pcDNA3-AMPKγ1; CA-AMPK, *right panel*) or the same amount of pcDNA3 empty plasmid (*left panel*). Cell extracts were obtained and analyzed as in *A*.

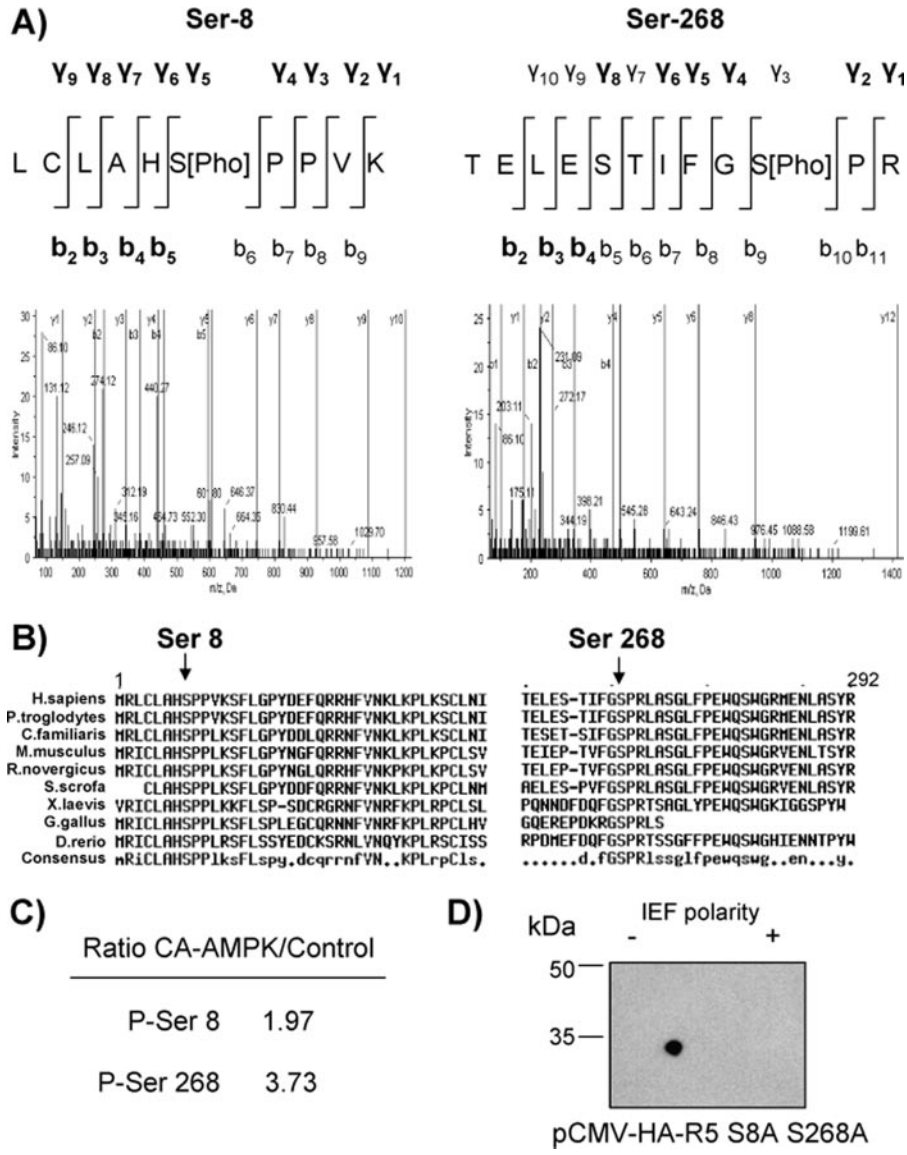

FIGURE 3. **AMPK induces the phosphorylation of residues Ser-8 and Ser-268 in R5/PTG.** *A*, 8×His-tagged R5/PTG purified from CHO cells was subjected to mass spectrometry analysis. Ions corresponding to phosphorylated residues are depicted in *boldface*. *B*, sequences corresponding to the N and C termini of R5/PTG sequences from different species (GenBank™) were aligned using the ClustalW program. The position of the Ser-8 and Ser-268 is indicated. *C*, 8×His-tagged R5/PTG was purified from CHO cells grown under conditions of AMPK activation by expressing a constitutively active form of AMPKγ1 (R70Q) subunit. The efficiency of the phosphorylation was compared with that obtained in CHO cells grown under standard conditions (see "Experimental Procedures"). *D*, cell extracts from CHO cells transfected with plasmid pCMV-HA-R5/PTG S8A S268A were analyzed by two-dimensional electrophoresis and Western blotting using anti-HA monoclonal antibodies.

RESULTS

R5/PTG Interacts Physically with and Is an in Vitro Target of AMPK—To study the possible functional relationship between AMPK and the glycogen targeting subunits of PP1, we analyzed, in a yeast two-hybrid system, the interaction between the different AMPK subunits and the PP1 glycogen targeting subunits G_M (PPP1R3), G_L (PPP1R4), and R5/PTG (PPP1R5) (1, 8). In the assays, we used the catalytic AMPKα2 subunit, the scaffolding AMPKβ2 subunit, and the regulatory AMPKγ1 subunit, because they are abundant in glycogenic tissues, such as liver and skeletal muscle (25, 26). As shown in Fig. 1*A*, we only detected a robust two-hybrid interaction between both the α2 catalytic and β2 regulatory subunits of the AMPK complex and the R5/PTG glycogen-targeting subunit. AMPKβ2 could also interact with G_L, although to a lesser extent. To confirm the interaction between AMPK subunits and R5/PTG, we expressed an Myc-tagged AMPKα2 subunit and an HA-tagged R5/PTG protein in mammalian HEK293 cells. Fig. 1*B* shows that when Myc-AMPKα2 was immunoprecipitated with anti-Myc antibodies, HA-R5/PTG was also recovered in the immunoprecipitates, suggesting a physical interaction between AMPKα2 and R5/PTG. These results were confirmed in mouse skeletal muscle crude extracts, where we found that endogenous AMPKα co-immunoprecipitated with endogenous R5/PTG when anti-R5/PTG antibodies were used in the assay (Fig. 1*C*).

Next, we studied whether as a consequence of the interaction between AMPK and R5/PTG, this latter protein was phosphorylated by the kinase. With this aim, we purified from bacteria a protein fusion of R5/PTG containing the maltose-binding protein (MBP) at its N terminus (MBP-R5/PTG). This protein was used in *in vitro* AMPK phosphorylation assays that demonstrated that AMPK was able to phosphorylate the MBP-R5/PTG fusion protein and that the presence of AMP (which activates AMPK) in the assay improved this phosphorylation (Fig. 1*D*). Control experiments with MBP alone showed no efficient phosphorylation by AMPK.

AMPK Modifies the in Vivo Phosphorylation Status of R5/PTG—It has been described that R5/PTG is a phosphoprotein whose basal level of phosphorylation does not change in response to insulin (which stimulates the Akt/PKB pathway), forskolin (that activates the PKA pathway), 12-*o*-tetradecanoylphorbol 13-acetate (which stimulates the PKC pathway), or epidermal growth factor (27, 28). We confirmed that R5/PTG is a phosphoprotein by two-dimensional electrophoresis and Western blotting of cell extracts from CHO cells transfected with plasmid pCMV-HA-R5/PTG. As shown in Fig. 2*A*, HA-R5/PTG fusion protein produced two major spots. The spot migrating faster toward the positive pole disappeared upon treatment of the sample with λ-phosphatase, indicating that this spot corresponded to phosphorylated forms of

HA-R5/PTG (Fig. 2*A*, see *arrow*). Interestingly, if the cells were treated with AICAR (an AMPK activator (29)), we obtained a different pattern of spots in the two-dimensional electrophoresis/Western blot. The faster migrating band disappeared, but a new band of lower isoelectric focusing mobility appeared close to the unphosphorylated form (Fig. 2*A*, *right panel*). Treatment of this sample with λ-phosphatase eliminated this intermediate form, suggesting that it was also phosphorylated (not shown). A similar pattern of the spots obtained upon AICAR treatment was observed if CHO cells were co-transfected with pCMV-HA-R5/PTG and a combination of plasmids that reconstituted a constitutively active form of the AMPK complex (CA-AMPK: pcDNA3-AMPKα2 T172D, pcDNA3-AMPKβ2, and pcDNA3-AMPKγ1) (Fig. 2*B*). These results suggested that the *in vivo* phosphorylation status of R5/PTG varied as a result of AMPK activation.

We next searched for putative AMPK phosphorylation consensus sites in the human R5/PTG protein sequence. We found that the sequences LKPLKS^{35}CLNI, DSKGLS^{69}LTAI, and AIHVFS^{77}DLPE closely fit with the consensus AMPK site, Hyd-(Basic,*X*)-*X*-*X*-Ser/Thr-*X*-*X*-*X*-Hyd, where Hyd can be Leu, Met, Ile, Phe, or Val, and Basic: Arg, Lys, or His (30). We mutagenized the corresponding Ser residues to Ala, but the mutated proteins produced the same pattern of *in vivo* phosphorylation (assessed by two-dimensional electrophoresis/western) as wild type (data not shown), indicating that none of these residues were true AMPK phosphorylation sites.

Then, we decided to identify the phosphorylation sites of R5/PTG by mass spectrometry. With this aim, we constructed a plasmid expressing R5/PTG with an N-terminal 8×His tag. This protein fusion was purified from CHO cells by Ni^{2+}-affinity chromatography, and phosphorylated residues were identified by mass spectrometry (see "Experimental Procedures"). In this way, in cells growing under standard growth conditions, we identified Ser-8 and Ser-268 as the major phosphorylated residues (Fig. 3*A*). These two residues, located at the N- and C-terminal part of the protein, respectively, are conserved in higher eukaryotes, from fish to human (Fig. 3*B*). We repeated the same determination in cells growing under conditions of AMPK activation by expressing a constitutively active form of the AMPKγ1 (R70Q) subunit. In this case, we did not identify additional phosphorylation sites, but we observed an increase in the extent of the phosphorylation of the previously identified Ser-8 and Ser-268 residues (Fig. 3*C*), indicating that these two sites were the major targets of AMPK action. Substitution of both Ser residues by Ala rendered a protein that showed a single spot by two-dimensional electrophoresis/Western analysis (similar results were obtained in cells growing under conditions of AMPK activation; not shown), indicating that no more phosphorylated residues were present in the double mutant (Fig. 3*D*).

Phosphorylation Status of R5/PTG Does Not Affect Its Interaction with Different Partners—We then tested the importance of the two phosphorylation sites of R5/PTG on the interaction of this glycogen targeting subunit with different partners, namely, the catalytic subunit of type 1 protein phosphatase (PP1c), the AMPKα2 and AMPKβ2 subunits of the AMPK complex (see above) and laforin, a dual specificity protein phosphatase involved in the Lafora disease (21). We observed that neither the Ser-8 → Ala nor the Ser-268 → Ala mutations affected the strength of the interaction between the R5/PTG-mutated forms and the different interaction partners (Fig. 4). Similar results were obtained when we assayed the Ser-8 → Asp and Ser-268 → Asp mutants, mimicking a constitutive negative charge in these residues (data not shown), indicating that the charge present at residues Ser-8 and Ser-268 did not affect the interaction with the assayed partners.

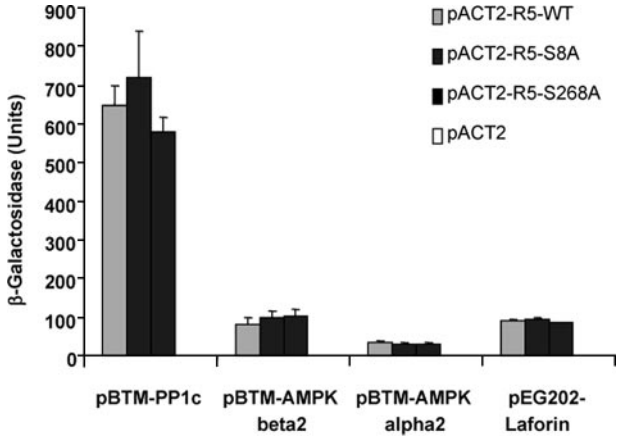

FIGURE 4. **Phosphorylation status of R5/PTG does not affect its interaction with different partners.** Yeast CTY10.5d cells transformed with plasmids pBTM-PP1c, pBTM-AMPKα2, pBTM-AMPKβ2, and pEG202-Laforin were co-transformed with plasmids pACT2 (empty), pACT2-R5/PTG wt, pACT2-R5/PTG S8A, and pACT2-R5/PTG S268A. Protein interaction was estimated using the yeast two-hybrid system, by measuring the β-galactosidase activity. Values correspond to means from four to six different transformants (*bars* indicate ± S.D.).

Phosphorylation Status of R5/PTG Affects Its Regulation by the Laforin-Malin Complex—We and others have recently described that the glycogenic activity and protein levels of R5/PTG were down-regulated by the complex formed by laforin (a dual specificity protein phosphatase) and malin (an E3-ubiquitin ligase), two proteins involved in the Lafora disease (see the introduction) (11–13). We measured then the glycogenic activity of the different mutants under control conditions and upon overexpression of the laforin-malin complex. In Hek293 cells, we observed that the glycogenic activity of the wild-type form of R5/PTG decreased in cells overexpressing the laforin-malin complex (Fig. 5*A*), similar to results reported for FTO2B hepatoma cells (12). The same result was obtained when the R5/PTG S268A mutant was assayed (Fig. 5*A*). However, the glycogenic activity of the R5/PTG S8A mutant was not affected by the overexpression of the laforin-malin complex (Fig. 5*A*).

These results could reflect a different susceptibility of the mutated forms of R5/PTG to be ubiquitinated by the laforin-malin complex and then targeted for proteasomal degradation. To study if this was the case, we analyzed the levels of the different R5/PTG forms in cells expressing laforin and increasing amounts of malin. As observed in Fig. 5*B*, the levels of wild-type R5/PTG decreased inversely to the levels of malin (a sign of its laforin-malin-induced degradation). R5/PTG S268A followed the same degradation profile as wild type (Fig. 5*B*) (similar results were obtained with the R5/PTG S268D mutant; not shown). However, in the case of R5/PTG S8A, the mutated

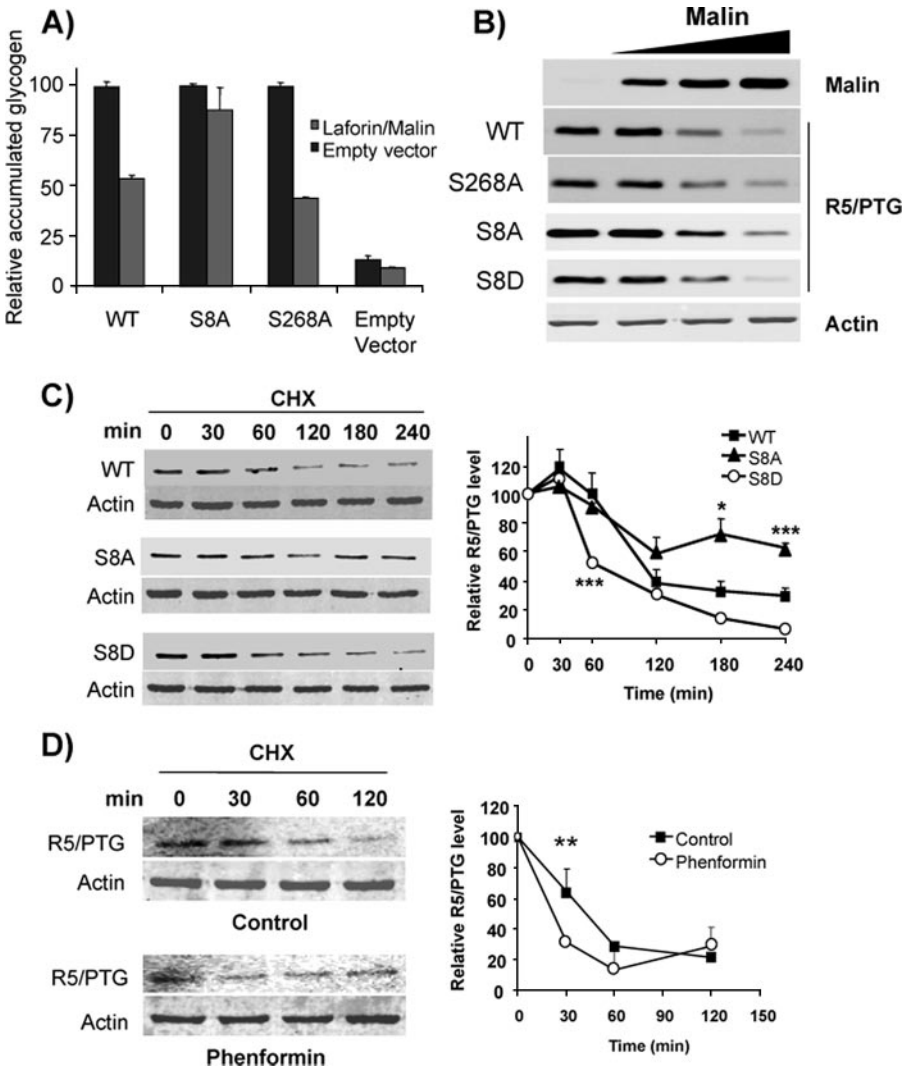

FIGURE 5. **Phosphorylation status of R5/PTG affects its regulation by the laforin/malin complex.** *A*, Hek293 cells were transfected with plasmids expressing the different mutated forms of R5/PTG (pCMV-HA-R5/PTG-derived plasmids) in combination or not with plasmids pCMV-Myc-Laforin and pcDNA-HA-Malin. Twenty-four hours after the transfection, the amount of glycogen was determined as described under "Experimental Procedures." *Bars* indicate ± S.D. of three independent experiments. *B*, degradation profiles of the different mutated forms of R5/PTG. Hek293 cells were co-transfected with pCMV-HA-R5/PTG-derived plasmids, pCMV-Myc-laforin, and different amounts of pcDNA-HA-Malin. Twenty-four hours after the transfection, cell extracts (25 μg) were analyzed by Western blot using anti-HA antibodies; anti-actin was used as loading control; a representative analysis is presented. *C*, degradation profiles of the different mutated forms of R5/PTG in the presence of cycloheximide. Hek293 cells were co-transfected with pCMV-Myc-laforin, pcDNA3-HA-Malin, and pCMV-HA-R5/PTG plasmids expressing the indicated proteins. Twenty-four hours after the transfection, cycloheximide (*CHX*, 100 μM) was added to the cultures, and cell extracts were analyzed by Western blotting at different times after the addition, using anti-HA and anti-actin antibodies (*left panel*); a representative analysis is presented. The relative intensity of the R5/PTG bands respect to the corresponding actin band was plotted as a function of time (*right panel*). *D*, degradation profile of R5/PTG in the presence of phenformin. Hek293 cells were co-transfected with pCMV-Myc-laforin, pcDNA3-HA-Malin, and pCMV-HA-R5/PTG plasmids as in *B*. Twenty-four hours after the transfection, cells were treated with 5 mM phenformin for 2 h, and then cycloheximide (*CHX*, 100 μM) was added to the cultures. Cell extracts were analyzed by Western blotting at different times after the addition, using anti-HA and anti-actin antibodies (*left panel*); a representative analysis is presented. The relative intensity of the R5/PTG bands respect to the corresponding actin band was plotted as a function of time (*right panel*).

protein was more resistant to the action of the laforin-malin complex, whereas an R5/PTG S8D mutant (mimicking a constitutively negative charge in this residue) showed an accelerated degradation (Fig. 5*B*).

To confirm these results, we examined the rate of R5/PTG degradation induced by the laforin-malin complex in the presence of cycloheximide (CHX), a protein synthesis inhibitor. As shown in Fig. 5*C*, the degradation of R5/PTG was prevented in the case of the S8A mutant, but accelerated in the case of the S8D mutant. These results suggested that phosphorylation of R5/PTG by AMPK increased its degradation by the laforin-malin complex. To confirm this hypothesis, we treated Hek293 cells with phenformin, a known activator of AMPK, and checked the rate of R5/PTG degradation induced by the laforin-malin complex in the presence of CHX, as above. As shown in Fig. 5*D*, treatment of the cells with phenformin increased the degradation rate of R5/PTG, indicating that activation of AMPK induces the degradation of R5/PTG by the laforin-malin complex. Fig. S1 (in the supplemental material) shows that phenformin treatment activated AMPK, and this resulted in an increase in the phosphorylation of acetyl-CoA carboxylase (a direct substrate of AMPK) and in an inactivation of the mammalian target of rapamycin pathway, reflected by a decrease in the phosphorylation of p70-S6 kinase; at the same time, endogenous levels of R5/PTG were diminished upon long term phenformin treatment.

As an additional proof of the involvement of the laforin-malin complex in the degradation of R5/PTG, we depleted Hek293 cells of endogenous laforin by small interference RNA silencing. We observed a marked increase in the levels of wild-type R5/PTG in laforin-depleted cells (Fig. 6*A*), confirming the role that the laforin-malin complex has in promoting the degradation of R5/PTG. We repeated the same experiment in cells expressing the R5/PTG S8A mutant and observed a higher accumulation of this form in comparison to wild type, indicating that phosphorylation of R5/PTG at Ser-8 improves its degradation (Fig. 6*A*). Because our results suggested a crucial role for the laforin-malin complex in the regulation of the glycogenic activity of R5/PTG, we postulated that in patients diagnosed with LD, lacking a functional laforin-malin complex, the down-regulation of R5/PTG would be deficient, leading to an accumulation of this protein. To test this hypothesis, we analyzed, by Western blotting, the levels of

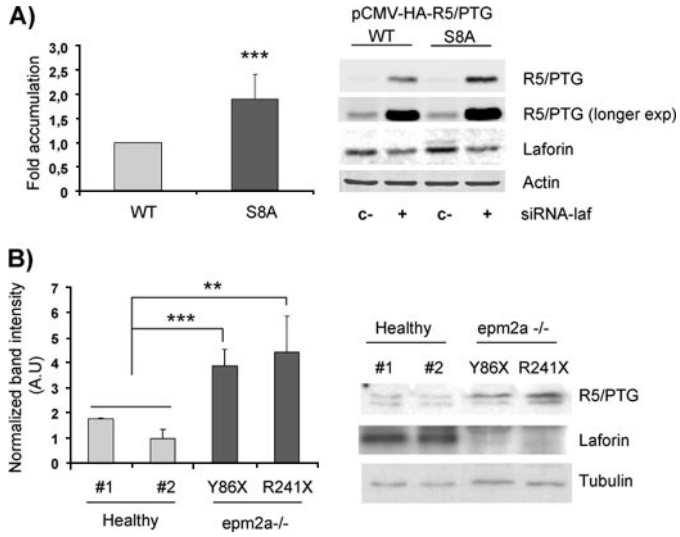

FIGURE 6. **Depletion of laforin increases the levels of R5/PTG.** *A*, Hek293 cells were co-transfected with plasmids pCMV-HA-R5/PTG (WT and S8A) and with 1 μg of pSUPER-laf plasmid expressing laforin small interference RNA (see "Experimental Procedures") or with an empty vector (*c-*). Twenty-four hours after the transfection, cells extracts (25 μg) were analyzed by Western blotting using anti-HA, anti-laforin, and anti-actin antibodies (*right panel*). A longer exposure of the blot with anti-HA was used to assess the levels of the proteins in the absence of laforin silencing; a representative analysis is presented. The relative intensity of the R5/PTG bands under control and laforin-depletion conditions in three independent experiments is plotted (*left panel*); *bars* indicate $\pm$ S.D. *B*, cell extracts from primary fibroblasts from two LD patients with mutations in the laforin gene (*epm2a*$^{-/-}$; Y86X and R241X) and from two healthy subjects (*#1* and *#2*) were analyzed by Western blotting using anti-R5/PTG and anti-laforin and anti-tubulin antibodies (*right panel*); a representative analysis is presented. The relative intensity of the R5/PTG bands with respect to the corresponding tubulin bands, in three independent experiments, is plotted (*left panel*); *bars* indicate $\pm$ S.D.

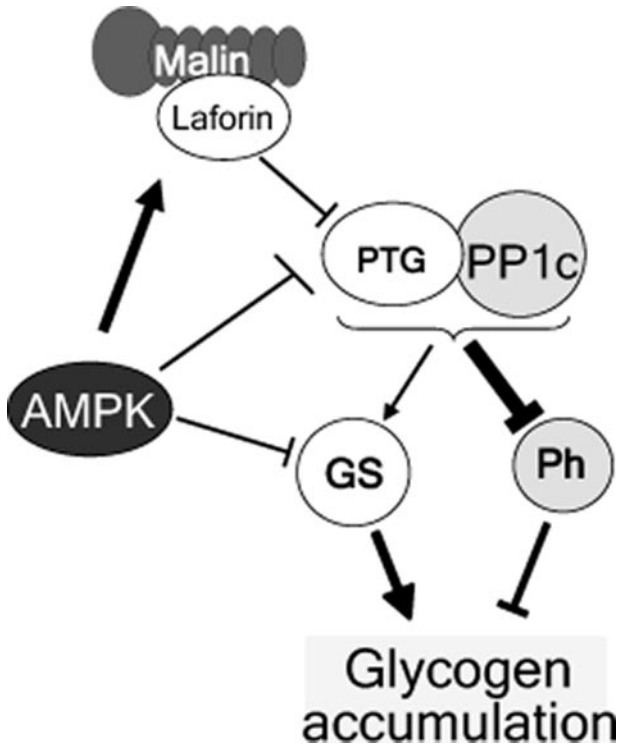

FIGURE 7. **Proposed role of AMPK on glycogen biosynthesis.** See text for details. *PP1c*, catalytic subunit of type 1 protein phosphatase; *GS*, glycogen synthase; and *Ph*, glycogen phosphorylase.

endogenous R5/PTG in extracts from primary fibroblasts from LD patients with mutations in the laforin gene (*epm2a*$^{-/-}$; Y86X and R241X nonsense mutations) and from healthy subjects. As shown in Fig. 6*B*, higher levels of endogenous R5/PTG were detected in the extracts from LD patients, confirming the importance of the laforin-malin complex in the regulation of R5/PTG.

DISCUSSION

Type 1 protein phosphatase (PP1) plays a prominent role in the regulation of glycogen homeostasis. PP1 is recruited to glycogen by a family of glycogen-targeting subunits that target the phosphatase to its glycogenic substrates. Because glycogen homeostasis is a crucial process, the activity of the holoenzyme formed by PP1 and one of these glycogenic-targeting subunits must be tightly regulated. In this work, we provide evidence elucidating the molecular mechanism by which the activity of one of these targeting subunits is regulated. We describe that the glycogenic activity of R5/PTG is regulated by phosphorylation, mediated by the AMP-activated protein kinase (AMPK); this kinase phosphorylates R5/PTG at two main sites, namely Ser-8 and Ser-268. At first glance, this regulation resembles that of G_M, another PP1-targeting subunit whose activity is down-regulated by PKA-dependent phosphorylation. However, and contrary to the effect produced by the phosphorylation of G_M, phosphorylation of R5/PTG does not interfere with its binding to PP1.

We and others have recently described that the glycogenic activity of R5/PTG is down-regulated by the laforin-malin complex, composed of a dual specificity protein phosphatase (laforin) and E3-ubiquitin ligase (malin) (11–13). Because R5/PTG interacted physically with laforin, but not with malin, we also suggested that laforin could recognize R5/PTG and recruit it to malin, which would then ubiquitinate the protein, targeting it for proteasomal degradation (12). We show in this work that phosphorylation of Ser-8 by AMPK accelerates the laforin-malin-dependent degradation of the protein. These results add a new role of AMPK in glycogen homeostasis, adding to its previously known action of phosphorylating and inactivating glycogen synthase both *in vitro* and *in vivo* (31, 32). In addition, these results complement our recent report that indicates that AMPK enhances the interaction between laforin and malin, resulting in an improved degradation of specific targets (12). In this way, AMPK not only improves the formation of a functional laforin-malin complex, but also makes R5/PTG a better substrate for the action of this degradative complex (Fig. 7). Because R5/PTG is expressed abundantly in adipocytes, skeletal muscle, heart, and liver (21), the regulatory mechanism described in this work could take place in all these tissues, which suggests an important role for this mechanism in the general homeostasis of glycogen.

Our results also add to our knowledge regarding the importance of the laforin-malin complex in glycogen biosynthesis. At present, it has been described that this complex is involved in the degradation of the muscle isoform of glycogen synthase (11), the glycogen debranching enzyme (amylo-1,6-glucosidase 4α-glucanotransferase) (33), and some glycogen-targeting subunits of PP1 such as R5/PTG (11–13) and R6 (13). These results,

taken together, suggest a crucial role of the laforin-malin complex in glycogen biosynthesis. In this work, we present evidence that depletion of laforin results in an increase in the levels of R5/PTG, indicating that this complex is a crucial negative regulator of at least this glycogen-targeting subunit. These results are in agreement with the important role that these two proteins play in the development of the Lafora disease (see the introduction). In LD patients lacking a functional laforin-malin complex, the down-regulation of R5/PTG would be deficient, leading to a more active R5/PTG-PP1 phosphatase holoenzyme that would stimulate glycogen accumulation. Consistent with this interpretation, in primary fibroblasts from LD patients with mutations in the laforin gene, we have observed higher levels of endogenous R5/PTG.

Recently, an alternative function of laforin on glycogen homeostasis has been described (34, 35). In this case, laforin acts as a phosphatase of complex carbohydrates, and it has been proposed that this function might be necessary for the maintenance of normal cellular glycogen. Our results are complementary to these observations, and, taken together, these results define the importance of the laforin-malin complex in regulating glycogen biosynthesis.

In conclusion, our work defines a novel mechanism for the regulation of glycogenic targeting subunits of PP1. In this case, the regulation is based on the phosphorylation of the regulatory subunit (R5/PTG) by AMPK, making it a better substrate for its laforin-malin-dependent degradation.

Acknowledgments—We thank Dr. David Brautigan for plasmid pcDNA3-FLAG-rabGM, Dr. D. Carling for the pcDNA3-AMPKα2 T172D, pcDNA3-AMPKβ2, and pcDNA3-AMPKγ1 plasmids, Dr. Libia Sanz (Instituto de Biomedicina de Valencia, Consejo Superior de Investigaciones Científicas) for the help in the two-dimensional electrophoresis, and Dr. Lynne Yenush for the critical reading of the manuscript.

REFERENCES

1. Roach, P. J. (2002) *Curr. Mol. Med.* **2,** 101–120
2. Ferrer, J. C., Favre, C., Gomis, R. R., Fernandez-Novell, J. M., Garcia-Rocha, M., de la Iglesia, N., Cid, E., and Guinovart, J. J. (2003) *FEBS Lett.* **546,** 127–132
3. Chen, Y. H., Hansen, L., Chen, M. X., Bjorbaek, C., Vestergaard, H., Hansen, T., Cohen, P. T., and Pedersen, O. (1994) *Diabetes* **43,** 1234–1241
4. Doherty, M. J., Moorhead, G., Morrice, N., Cohen, P., and Cohen, P. T. (1995) *FEBS Lett.* **375,** 294–298
5. Doherty, M. J., Young, P. R., and Cohen, P. T. (1996) *FEBS Lett.* **399,** 339–343
6. Armstrong, C. G., Browne, G. J., Cohen, P., and Cohen, P. T. (1997) *FEBS Lett.* **418,** 210–214
7. Munro, S., Ceulemans, H., Bollen, M., Diplexcito, J., and Cohen, P. T. (2005) *FEBS J.* **272,** 1478–1489
8. Newgard, C. B., Brady, M. J., O'Doherty, R. M., and Saltiel, A. R. (2000) *Diabetes* **49,** 1967–1977
9. Aggen, J. B., Nairn, A. C., and Chamberlin, R. (2000) *Chem. Biol.* **7,** R13–R23
10. Cohen, P. T. (2002) *J. Cell Sci.* **115,** 241–256
11. Vilchez, D., Ros, S., Cifuentes, D., Pujadas, L., Valles, J., Garcia-Fojeda, B., Criado-Garcia, O., Fernandez-Sanchez, E., Medrano-Fernandez, I., Dominguez, J., Garcia-Rocha, M., Soriano, E., Rodriguez de Cordoba, S., and Guinovart, J. J. (2007) *Nat. Neurosci.* **10,** 1407–1413
12. Solaz-Fuster, M. C., Gimeno-Alcaniz, J. V., Ros, S., Fernandez-Sanchez, M. E., Garcia-Fojeda, B., Criado Garcia, O., Vilchez, D., Dominguez, J., Garcia-Rocha, M., Sanchez-Piris, M., Aguado, C., Knecht, E., Serratosa, J., Guinovart, J. J., Sanz, P., and Rodriguez de Cordoba, S. (2008) *Hum. Mol. Genet.* **17,** 667–678
13. Worby, C. A., Gentry, M. S., and Dixon, J. E. (2008) *J. Biol. Chem.* **283,** 4069–4076
14. Ganesh, S., Puri, R., Singh, S., Mittal, S., and Dubey, D. (2006) *J. Hum. Genet.* **51,** 1–8
15. Francois, J., and Parrou, J. L. (2001) *FEMS Microbiol. Rev.* **25,** 125–145
16. Hardy, T. A., Huang, D., and Roach, P. J. (1994) *J. Biol. Chem.* **269,** 27907–27913
17. Hardie, D. G., and Sakamoto, K. (2006) *Physiology* (*Bethesda*) **21,** 48–60
18. Hardie, D. G. (2007) *Nat. Rev.* **8,** 774–785
19. Liu, J., Wu, J., Oliver, C., Shenolikar, S., and Brautigan, D. L. (2000) *Biochem. J.* **346,** 77–82
20. Legrain, P., Dokhelar, M.-C., and Transy, C. (1994) *Nucleic Acids Res.* **22,** 3241–3242
21. Fernandez-Sanchez, M. E., Criado-Garcia, O., Heath, K. E., Garcia-Fojeda, B., Medrano-Fernandez, I., Gomez-Garre, P., Sanz, P., Serratosa, J. M., and Rodriguez de Cordoba, S. (2003) *Hum. Mol. Genet.* **12,** 3161–3171
22. Solaz-Fuster, M. C., Gimeno-Alcaniz, J. V., Casado, M., and Sanz, P. (2006) *Cell. Signal.* **18,** 1702–1712
23. Ludin, K., Jiang, R., and Carlson, M. (1998) *Proc. Natl. Acad. Sci. U. S. A.* **95,** 6245–6250
24. Chan, T. M., and Exton, J. H. (1976) *Analyt. Biochem.* **71,** 96–105
25. Thornton, C., Snowden, M. A., and Carling, D. (1998) *J. Biol. Chem.* **273,** 12443–12450
26. Winder, W. W. (2001) *J. Appl. Physiol.* **91,** 1017–1028
27. Brady, M. J., Printen, J. A., Mastick, C. C., and Saltiel, A. R. (1997) *J. Biol. Chem.* **272,** 20198–20204
28. Printen, J. A., Brady, M. J., and Saltiel, A. R. (1997) *Science* **275,** 1475–1478
29. Corton, J. M., Gillespie, J. G., Hawley, S. A., and Hardie, D. G. (1995) *Eur. J. Biochem.* **229,** 558–565
30. Hardie, D. G., Scott, J. W., Pan, D. A., and Hudson, E. R. (2003) *FEBS Lett.* **546,** 113–120
31. Carling, D., Clarke, P. R., Zammit, V. A., and Hardie, D. G. (1989) *Eur. J. Biochem.* **186,** 129–136
32. Jorgensen, S. B., Nielsen, J. N., Birk, J. B., Olsen, G. S., Viollet, B., Andreelli, F., Schjerling, P., Vaulont, S., Hardie, D. G., Hansen, B. F., Richter, E. A., and Wojtaszewski, J. F. (2004) *Diabetes* **53,** 3074–3081
33. Cheng, A., Zhang, M., Gentry, M. S., Worby, C. A., Dixon, J. E., and Saltiel, A. R. (2007) *Genes Dev.* **21,** 2399–2409
34. Worby, C. A., Gentry, M. S., and Dixon, J. E. (2006) *J. Biol. Chem.* **281,** 30412–30418
35. Tagliabracci, V. S., Turnbull, J., Wang, W., Girard, J. M., Zhao, X., Skurat, A. V., Delgado-Escueta, A. V., Minassian, B. A., Depaoli-Roach, A. A., and Roach, P. J. (2007) *Proc. Natl. Acad. Sci. U. S. A.* **104,** 19262–19266